Identification of Seismic Ground Motions in a Near-Surface 2D Domain Subject to Unknown SH Incident Waves

Bruno P. Guidio, Ph.D.[1] and Chanseok Jeong, Ph.D.[1]

[1]School of Engineering and Technology, Central Michigan University, Mount Pleasant, MI 48859, USA; E-mail: peruq1b@cmich.edu & jeong1c@cmich.edu (corresponding author)

ABSTRACT

A new inversion approach for estimating the shear wave motions in an interior domain surrounded by the domain reduction method (DRM) layer from sparsely-measured seismic motion data is presented in this paper. We consider a 2D domain truncated by wave-absorbing boundary conditions (WABC), and the DRM is utilized to inject incident waves into the domain. We attempt to identify an effective seismic force at the DRM layer and reconstruct the ground motions in an interior domain. A gradient-based minimization method minimizes a misfit between measured motions induced by targeted effective forces and their estimated counterparts. The numerical results show that targeted ground motions in an interior domain can be reconstructed. To accurately reconstruct the wave responses, a minimum sensor spacing is required, and it clearly depends on the dominant frequency of incident waves.

INTRODUCTION

In the area of earthquake engineering, there is a need to relate measured seismic data to ground motions in a near-surface domain of interest. By doing so, engineers could identify the locations where responses of large amplitudes took place during a seismic event and investigate the impact of earthquakes on critical structures, including subsurface systems (foundations and underground structures) and their surrounding soils. Therefore, such a method can contribute to examining the weak points (e.g., possible locations of structural failures) of critical infrastructure shortly after a seismic event, and, thus, making it possible to judge whether the infrastructure is structurally sound to reuse after the earthquake.

To date, there have been two dominant, conventional methods for the identification of incident seismic waves that hit a near-surface domain: one is deconvolution in a one-dimensional (1D) setting (Mejia and Dawson, 2006; Poul and Zerva, 2018a,b) and the other is the inversion of a seismic source profile at a fault in a very large (e.g., hundreds of kilometers long) regional-scale domain (Akcelik et al., 2002). As an alternative to such conventional methods, this paper presents a new numerical method to identify arbitrary, incoherent incoming seismic waves and reconstruct corresponding wave responses in a truncated multi-dimensional domain by using sparsely measured ground motion.

The PDE-constrained optimization has advanced the inverse problems associated with elastodynamic wave motions, and the associated applications span from material characterization to dynamic-input identification or optimization. For instance, geotechnical site material characterization has been investigated by using the PDE-constrained optimization (Fathi el al.,

2015; Fathi et al., 2016; Jeong et al., 2009; Kang and Kallivokas, 2010; Tran and McVay, 2012). The approach has been used for studying wave-source optimization in consideration of complex geological formations (Jeong et al 2015; Jeong and Kallivokas 2016). To investigate the feasibility to identify arbitrary, incoherent incoming seismic waves in a truncated domain by using sparse seismic measurement by using the PDE-constrained optimization framework, Jeong and Seylabi (2018) and Guidio and Jeong (2021) studied a full-waveform source-inversion method to identify an incoming seismic wave in a 1D semi-infinite solid and a 2D bounded domain, respectively. Guidio et al. (2021) also discussed a numerical method that can reconstruct the comprehensive profiles (i.e., both spatial and temporal distributions) of complex, incoherent seismic incident wavefields, modeled as traction on WABC, propagating into a 2D truncated domain of anti-plane shear wave motion without using any regularization. Lloyd and Jeong (2018) presented an approach to identifying the spatial and temporal distributions of moving wave sources in a solid.

Continuing the aforementioned works, the presented paper extends the aforementioned works in consideration of DRM physics for the primary purpose of reconstructing the ground motions in a domain surrounded by a DRM layer and WABC.

PROBLEM DEFINITION

The presented method is aimed at (*i*) identifying an effective seismic force on the DRM layer as an incident seismic motion that allows its corresponding wave responses to match the measured motions at sensor locations on the ground surface and (*ii*) consequently reconstructing wave responses in an interior domain surrounded by the DRM layer. This work considers a two-dimensional heterogeneous domain of anti-plane shear wave motions as shown in Figure 1.

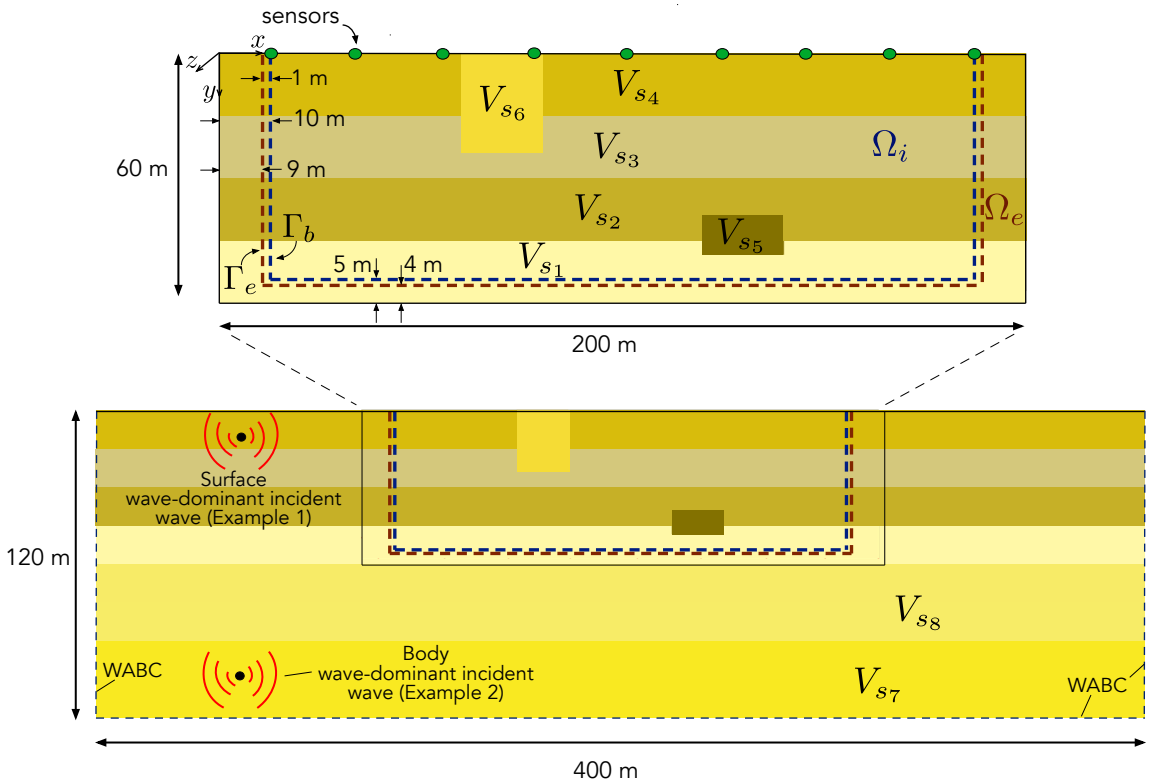

Figure 1. Problem configuration. (Upper) a DRM-ABC-truncated domain used for an inversion solver; (Lower) an enlarged domain used for generating targeted wave responses.

Governing wave physics. The strong form of the governing differential equation for the shear wave propagation in the domain Ω is:

$$\nabla.(G\nabla u) - \rho\frac{\partial^2 u}{\partial t^2} = 0, \tag{1}$$

where $u = u(x, y, t)$ denotes the displacement field of wave motions in the z-plane, which is perpendicular to the direction that the wave is moving; x and y denote horizontal and vertical coordinates; $G(x, y)$ and $\rho(x, y)$ denote the shear modulus and the mass density of the solid.

The traction-free condition is presented on the top surface, while the absorbing boundary conditions (Lysmer and Kuhlemeyer, 1969) are presented on the left, bottom, and right boundaries. The zero initial-value conditions are presented as the system is initially at rest.

Please note that the information on a targeted incident wave motion is not included in this strong form. The information on a target incident wave will be included in the global force vector per the DRM theory of a discrete form. Then, using the finite element method the strong form turns to the following semi-discrete equation:

$$\mathbf{M}\ddot{\mathbf{u}}(t) + \mathbf{C}\dot{\mathbf{u}}(t) + \mathbf{K}\mathbf{u}(t) = \mathbf{F}(t) \tag{2}$$

where $\mathbf{u}(t)$, $\dot{\mathbf{u}}(t)$, and $\ddot{\mathbf{u}}(t)$ denote the displacement, velocity, and acceleration vectors of the state problem at time t, respectively. **K**, **C**, and **M** denote the global stiffness, damping, and mass matrices, respectively, while $\mathbf{F}(t)$ is the global force vector.

Domain reduction method (DRM). In Bielak's DRM formulation (Bielak et al., 2003; Yoshimura et al., 2003), the semi-infinite solid is subdivided into three different parts: the interior domain Ω_i, an interface Γ_b, and the exterior domain Ω_e, as shown in the upper figure in Figure 1. Besides, the subscripts *i*, *b*, and *e* are used to denote the nodes on the interior domain of interest, interface, and exterior domain, respectively. The nodes on Γ_b, and their neighboring exterior nodes, localized at the fictitious boundary Γ_e, form the DRM layer. Per the DRM theory, a targeted effective seismic force vector $\mathbf{F}^{\text{eff}}$, obtained from free-field ground motions, is applied on all the nodes on the DRM layer in order to consistently model incident seismic waves impinging the domain. Bielak's DRM formulation shows how only the free-field displacements and acceleration, $\mathbf{u}^0$ and $\ddot{\mathbf{u}}^0$, respectively, at nodes of the DRM layer are utilized to determine the effective seismic force vector $\mathbf{F}^{\text{eff}}$. Then, in the presented approach, $\mathbf{F}(t)$is replaced by $\mathbf{F}^{\text{eff}}$.

Discrete state problem. The time-dependent semi-discrete equation is solved by considering the initial-value conditions and applying the implicit Newmark time integration. Then, the state problem is formed in the compact form, $\mathbf{Q}\hat{\mathbf{u}} = \hat{\mathbf{F}}$, where matrix **Q**, solution vector $\hat{\mathbf{u}}$, and global force vector $\hat{\mathbf{F}}$, are all defined as shown in the authors' previous work (Guidio et al., 2021).

INVERSE MODELING

Under this inversion method, we determine the control parameters as $P_{b_{kj}}$ and $P_{e_{kj}}$. They are components of estimated force vector, $\hat{\mathbf{F}}_{\text{estm}}$, corresponding to γ_{b_k} and γ_{e_k} , respectively, and t_j:

γ_{b_k} is the k-th discrete node on the DRM boundary, and γ_{e_k} is the k-th discrete node on; and t_j is the j-th time step.

Discrete objective and Lagrangian functional. We attempt to determine the values of control parameters that minimize the discrete objective functional, which is defined as:

$$\hat{\mathcal{L}} = 0.5\,(\hat{\mathbf{u}} - \hat{\mathbf{u}}_{\mathrm{m}})^T\,\overline{\mathbf{B}}\,(\hat{\mathbf{u}} - \hat{\mathbf{u}}_{\mathrm{m}}), \tag{3}$$

where $\hat{\mathbf{u}}$ and $\hat{\mathbf{u}}_{\mathrm{m}}$ are obtained by a set of targeted and estimated control parameters, respectively, and $\overline{\mathbf{B}}$ is defined as $\Delta t\mathbf{B}$, where $\mathbf{B}$ a square matrix, of which components are all 0 except for those of the diagonal, having values of all 1, if they correspond to the degrees of freedom at sensor locations.

By imposing state equation onto an objective functional by using the Lagrangian multiplier vector $\hat{\boldsymbol{\lambda}}$, we cast the following Lagrangian functional:

$$\hat{\mathcal{A}} = \mathbf{0.5}(\hat{\mathbf{u}} - \hat{\mathbf{u}}_{\mathrm{m}})^T\,\overline{\mathbf{B}}\,(\hat{\mathbf{u}} - \hat{\mathbf{u}}_{\mathrm{m}}) - \hat{\boldsymbol{\lambda}}^T\left(\mathbf{Q}\hat{\mathbf{u}} - \hat{\mathbf{F}}_{\mathrm{estm}}\right), \tag{4}$$

where $\hat{\mathbf{F}}_{\mathrm{estm}}$ is the estimated force vector.

Optimally conditions. To identify unknown target control parameters, the first-order optimality conditions should be fulfilled. The first condition, $(\partial\hat{\mathcal{A}}/\partial\hat{\boldsymbol{\lambda}}) = 0$, will be automatically satisfied when we solve the discrete forward problem.

The second condition, $(\partial\hat{\mathcal{A}}/\partial\hat{\mathbf{u}}) = 0$, will be automatically satisfied when the adjoint problem is solved. We have shown how to solve an adjoint problem of the same form by marching backward in time in our previous work (Guidio et al, 2021).

The third condition will be satisfied when we solve the control problem, $(\partial\hat{\mathcal{A}}/\partial\hat{\mathbf{F}}_{\mathrm{estm}}) = \hat{\boldsymbol{\lambda}} = 0$, which implies that a gradient vector, $\partial\hat{\mathcal{A}}/\partial\hat{\mathbf{F}}_{\mathrm{estm}} = \partial\,\hat{\mathcal{L}}/\partial\hat{\mathbf{F}}_{\mathrm{estm}}$, is comprised of the component of the vector $\hat{\boldsymbol{\lambda}}$ corresponding to the global node numbering and time step of control parameters.

Control parameters updates. By using the semi-analytical evaluated, gradient vector, this work iteratively updates the estimated control parameters as follows. First, the conjugate-gradient method determines the best search direction, and an optimal step length is calculated by Newton's method (Guidio and Jeong, 2021). Then, the gradient-based minimization scheme updates the control parameters by summing the previous control parameters and the product between the search direction and optimal step length. We perform the numerical experiments of the presented inversion method by using our in-house forward and inverse wave solver written in MATLAB (Some or all data, models, or code generated or used during the study are available from the authors by request).

NUMERICAL EXPERIMENTS

In this section, two numerical experiments are considered where the ground motions are induced by a 2D free-field wave generator in an enlarged domain, shown at the bottom of Figure 1. Its dimension is 400 m x 120 m, and the shear wave speeds are V_{s_1}= 300 m/s, V_{s_2}= 250 m/s, V_{s_3}= 200 m/s, V_{s_4}= 150 m/s, V_{s_5}= 800 m/s, V_{s_6}= 1000 m/s, V_{s_7}= 1800 m/s, and V_{s_8}= 1500 m/s. The mass density is 1500 kg/m³, and it is uniform in the entire domain. We note that the DRM-ABC-

truncated domain that is used during the inversion process is incorporated into the enlarged domain, as shown in the upper figure in Figure 1.

The first example studies the performance of the presented inversion solver for reconstructing $\hat{\mathrm{F}}^{\mathrm{eff}}$ and the surface wave-dominant ground motions induced by surface wave-dominant incident waves, which are generated by a 2D free-field wave generator using the enlarged domain. The second example is focused on examining the inversion performance to reconstruct body wave-dominant ground motions produced by incoherently-propagating body wave-dominant incident waves.

The accuracy to reconstruct the ground motions in Ω_i is appraised by using the following error norm between the ground motions at the j-th time step induced by targeted effective force vector, $\mathrm{u}_{\mathrm{m}_j}^{\mathrm{interior}}$, and their reconstructed counterparts, $\mathrm{u}_j^{\mathrm{interior}}$:

$$\varepsilon^u = \sum_{j=1}^{N} \frac{\left|\mathrm{u}_{\mathrm{m}_j}^{\mathrm{interior}} - \mathrm{u}_j^{\mathrm{interior}}\right|^2}{\left|\mathrm{u}_{\mathrm{m}_j}^{\mathrm{interior}}\right|^2} \ [\%]. \tag{5}$$

Example 1: Examining the inversion performance to reconstruct surface wave-dominant ground motions

This example studies the performance of estimating the effective seismic force at the DRM layer and the ground motions generated by incoherently-propagating surface wave-dominant incident waves. To create the incident waves, the FEM free-field generator uses a point wave source, located in the top-left area in the enlarged domain shown in the lower figure of Fig. 1, and its source time signal is characterized by a Ricker wavelet signal.

Figure 2 shows the relation among ε^u, the sensor spacing, and the dominant frequency of the seismic incident waves. As shown in Figure 12, the inversion solver can effectively reconstruct the targeted wave responses within the interior domain Ω_i for surface wave-dominant incident waves of the central frequency of 2 Hz by using a sensor spacing of up to 30 m, to achieve ε^u less than 5%. However, for a surface wave-dominant incident wave of the central frequency of 5 Hz and 10 Hz, the maximum required sensor spacings are 10 m and 5 m, respectively, to achieve ε^u less than 5%.

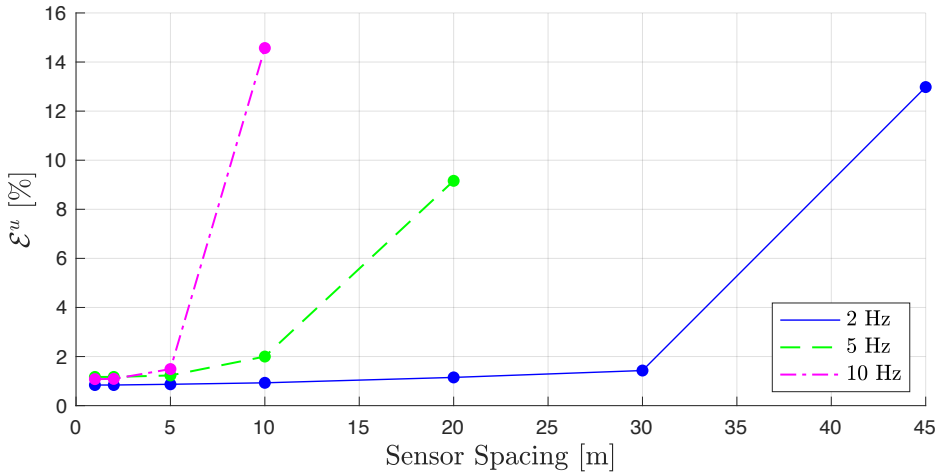

Figure 2. Relation between the sensor spacing and the dominant frequency of a surface wave-dominant incident wave.

Figure 3 shows the ground motions induced by targeted and reconstructed effective forces in the case, in which a Ricker signal of a central frequency of 10 Hz is used as the wave source signal in the 2D free-field wave generator. We note that the top row of Figure 3 shows the targeted wave responses computed in the entire domain but shown only in Ω_i surrounded by the DRM layer. Figure 3 reveals the gradual decrement of agreement between the targeted and reconstructed wave responses in Ω_i as the spacing of the sensors is increased.

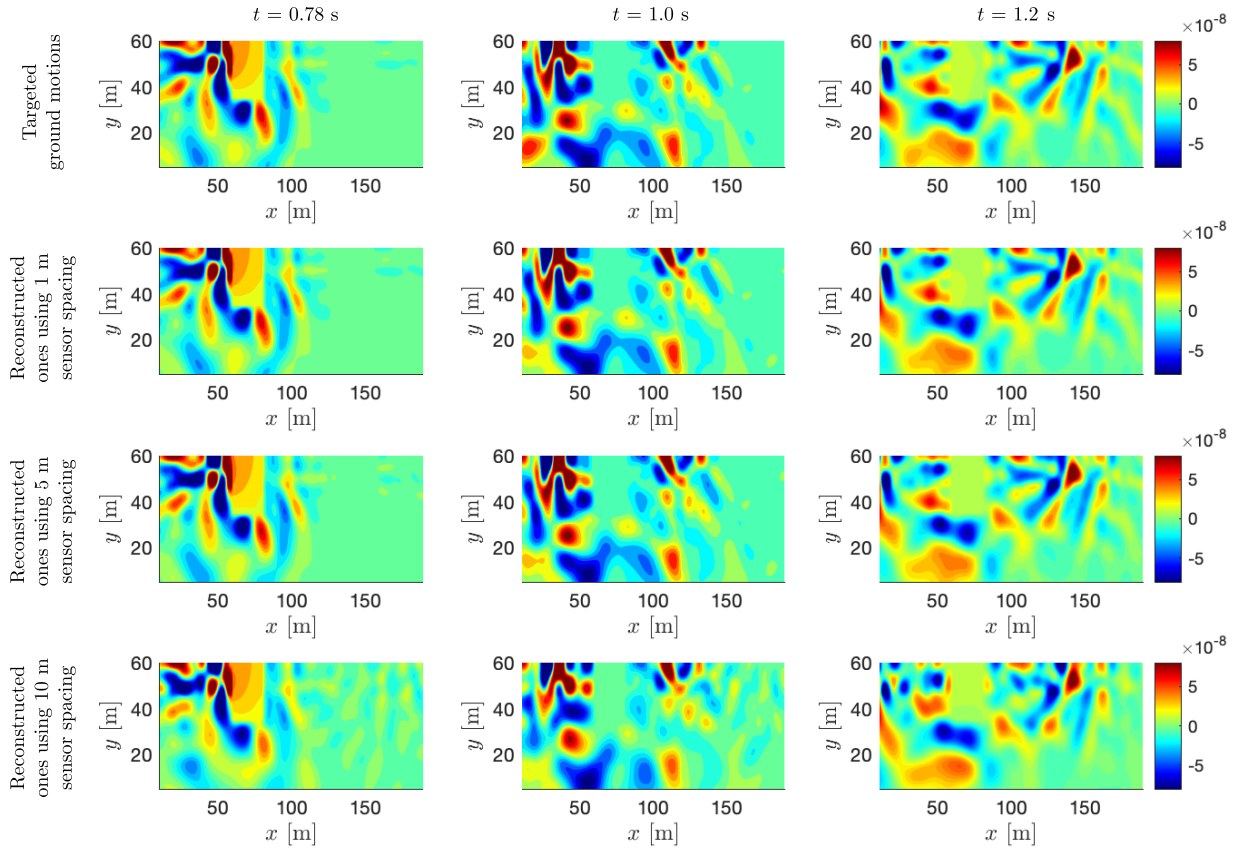

Figure 3. Targeted wave responses in an interior domain Ω_i induced by surface wave-dominant incident waves, which are initialized by a source with a dominant frequency of 10 Hz; and their reconstructed counterparts using 1 m, 5 m, and 10 m sensor spacing.

Example 2: Investigating the inversion performance to reconstruct body wave-dominant ground motions

This example is focused on examining the performance of the presented inversion solver for reconstructing the body wave-dominant ground motions in Ω_i induced by incoherently-propagating body wave-dominant free-field waves. A point wave source characterized by a Ricker wavelet and located at the bottom-left of the enlarged domain is utilized in this example to generate targeted wave responses.

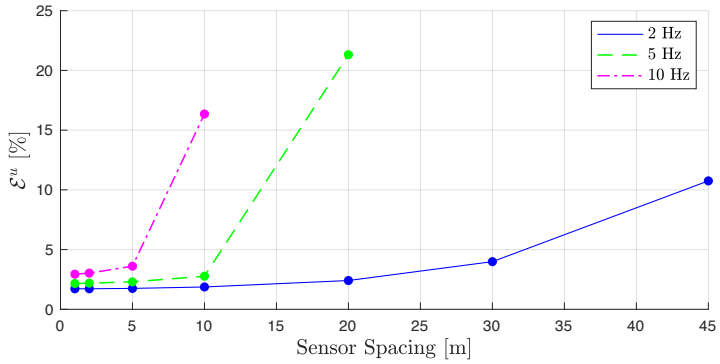

Figure 4. Relation between the sensor spacing and the dominant frequency of a body wave-dominant incident wave.

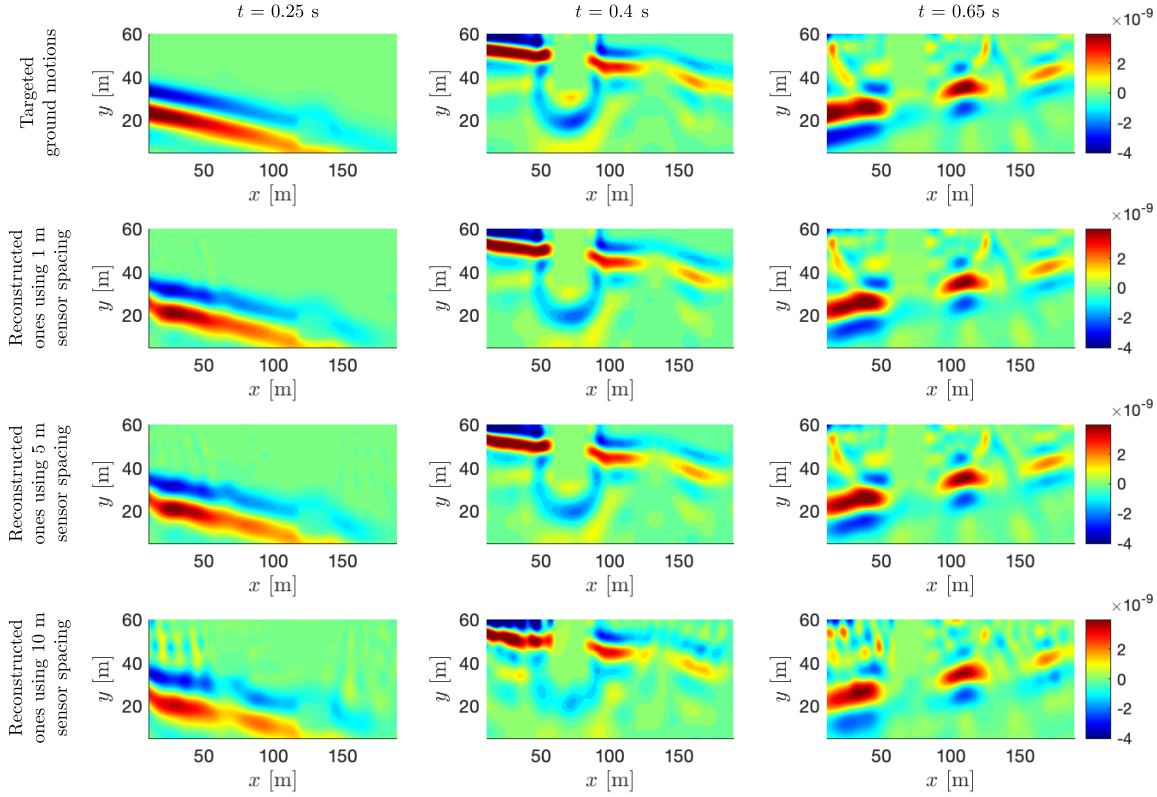

Figure 5. Targeted wave responses in Ω_i induced by body wave-dominant incident waves, which are initialized by a source with a dominant frequency of 10 Hz; and their reconstructed counterparts using 1 m, 5 m, and 10 m sensor spacing.

Figure 4 shows the sensor spacing required to adequately reconstruct the ground motions in Ω_i. Namely, a less dense array of sensors is needed to properly estimate body wave-dominant ground motions with a lower dominant frequency.

In Figure 5, we present the case in which a Ricker wavelet with a 10 Hz dominant frequency is used for a wave source signal in the free-field modeling. Figure 6 shows the gradually increasing

mismatch between the targeted ground motions and their reconstructed counterparts as the spacing of sensors on the surface increase.

Therefore, this example shows that the presented inverse solver can effectively reconstruct body wave-dominant ground motions, provide that the sensor spacing is adequately set in consideration of the dominant frequency of the incident wave.

CONCLUSION

In this study, we discussed a new method to (*i*) identify an effective seismic force on a DRM layer as an incident seismic motion and (*ii*) reconstruct wave responses in the interior domain from sparsely-measured seismic data in a 2D domain truncated by WABC. Specifically, the DRM is used to model incident waves into the domain, gradient-based minimization is utilized to tackle the inverse problem, and the DTO approach is employed to solve the adjoint problem. It was shown that the wave responses in an interior domain surrounded by a DRM layer can be reconstructed by using the presented method. Lastly, a minimum spacing of sensors is needed to reconstruct the ground motions, and it depends on the dominant frequency of the incident waves.

If the presented method is extended to 3D settings, it may be used by geotechnical earthquake engineers to replay the ground motions in a near-surface domain caused by an earthquake in a fine resolution over space and time. Namely, sensors (e.g., accelerometers, vision sensors, or optical cables) can measure the vibrational motions around an infrastructure under consideration. Then, the presented method will turn the sparsely measured motion data into the wave responses in the infrastructure and surrounding soils. Based on such estimated responses, engineers can accurately pinpoint superstructures or underground structures that were damaged or impacted during an earthquake. Thus, the presented method can help engineers or policymakers make decisions and plan budgets on structural repairs.

ACKNOWLEDGMENT

This material is based upon work supported by the National Science Foundation under Award CMMI-1855406 and CMMI-2044887. Any opinions, findings, and conclusions or recommendations expressed in this material are those of the authors and do not necessarily reflect the views of the National Science Foundation. The authors are also grateful for the support by the Faculty Research and Creative Endeavors (FRCE) Research Grant 48058 at Central Michigan University.

REFERENCES

Akcelik, V., Biros, G., Ghattas, O. (2002). “Parallel multiscale Gauss-Newton-Krylov methods for inverse wave propagation, in: Supercomputing” ACM/IEEE 2002 Conference.

Bielak, J., Loukakis, K., Hisada, Y., Yoshimura, C. (2003). “Domain reduction method for three-dimensional earthquake modeling in localized regions, Part I: Theory.” *Bulletin of Seismological Society of America*, 93, 817-824.

Fathi, A., Kallivokas, L.F., Poursartip, B. (2015). “Full-waveform inversion in three-dimensional PML-truncated elastic media.” *Computer Methods in Applied Mechanics and Engineering,* 296, 39-72.

Fathi, A., Poursartip, B., Stokoe II, K.H., Kallivokas, L.F. (2016). "Three-dimensional P- and S-wave velocity profiling of geotechnical sites using full-waveform inversion driven by field data." *Soil Dynamics and Earthquake Engineering*, 87, 63-81

Guidio, B., Jeremic, B., Guidio, L.P., Jeong, C. (2021). "Passive-seismic inversion of sh-wave input motions in a domain truncated by wave absorbing boundary condition." (under review).

Guidio, B.P., Jeong, C. (2021). "Full-waveform inversion of incoherent dynamic traction in a bounded 2d domain of scalar wave motions." *Journal of Engineering Mechanics*, 147, 10.1061/(ASCE)EM.1943-7889.0001909, 04021010.

Jeong, C., Na, S.W., Kallivokas, L.F. (2009). "Near-surface localization and shape identification of scatterer embedded in a halfplane using scalar waves." *Journal of Computational Acoustics*, 17, 277-308.

Jeong, C., Kallivokas, L., Kucukcoban, S., Deng, W., Fathi, A. (2015). "Maximization of wave motion within a hydrocarbon reservoir for wave-based enhanced oil recovery." *Journal of Petroleum Science and Engineering*, 129, 205–220.

Jeong, C., Kallivokas, L.F. (2016). "An inverse-source problem for maximization of pore-fluid oscillation within poroelastic formations." *Inverse Problems in Science and Engineering*, 25.

Jeong, C., Seylabi, E.E. (2018). "Seismic input motion identification in a heterogeneous halfspace." *Journal of Engineering Mechanics*, 144, no. 8: 04018070.

Kang, J.W., Kallivokas, L.F. (2010). "The inverse medium problem in 1D pml-truncated heterogeneous semi-infinite domains." *Inverse Problems in Science and Engineering,* 18, 759-786.

Lloyd, S. F., C. Jeong. (2018). "Adjoint equation-based inverse-source modeling to reconstruct moving acoustic sources in a one-dimensional heterogeneous solid." *Journal of Engineering Mechanics,* 144, no. 9: 04018089.

Lysmer, J., Kuhlemeyer, R.L. (1969). "Finite dynamic model for infinite media." *Journal of Engineering Mechanics Division ASCE*, 95, 859–877.

Mejia, L., Dawson, E. (2006). "Earthquake deconvolution for FLAC". *FLAC and Numerical.*

Poul, M.K., Zerva, A. (2018a). "Efficient time-domain deconvolution of seismic ground motions using the equivalent-linear method for soil-structure interaction analyses." *Soil Dynamics and Earthquake Engineering*, 112, 138 – 151.

Poul, M.K., Zerva, A., (2018b). "*Nonlinear dynamic response of concrete gravity dams considering the deconvolution process.*" Soil Dynamics and Earthquake Engineering, 109, 324 – 338.

Tran, K.T., McVay, M. (2012). "Site characterization using Gauss-Newton inversion of 2-D full seismic waveform in the time domain." *Soil Dynamics and Earthquake Engineering,* 43, 16-24.

Yoshimura, C., Bielak, J., Hisada, Y., Fernández, A. (2003). "Domain reduction method for three dimensional earthquake modeling in localized regions, Part II: Verification and applications." *Bulletin of the Seismological Society of America*, 93, 825-841.